

NANO-CHEMICALLY MODIFIED TETRACYCLINE-3 (nCMT-3) ATTENUATES ACUTE LUNG INJURY VIA BLOCKING sTREM-1 RELEASE AND NLRP3 INFLAMMASOME ACTIVATION

Qinghe Meng,* Xiaojing Wang,[†] Dandan Guo,[†] Changying Shi,[†] Raymond Gu,* Julia Ma,* Gary Nieman,*[‡] Michaela Kollisch-Singule,*[‡] Juntao Luo,*^{†‡} and Robert N. Cooney*[‡]

*Department of Surgery, State University of New York (SUNY), Upstate Medical University, Syracuse, New York; [†]Department of Pharmacology, State University of New York (SUNY), Upstate Medical University, Syracuse, New York; and [‡]Sepsis Interdisciplinary Research Center (SIRC), State University of New York (SUNY), Upstate Medical University, Syracuse, New York

Received 6 Jan 2022; first review completed 31 Jan 2022; accepted in final form 8 Mar 2022

ABSTRACT—Background: Intratracheal (IT) lipopolysaccharide (LPS) causes severe acute lung injury (ALI) and systemic inflammation. CMT-3 has pleiotropic anti-inflammatory effects including matrix metalloproteinase (MMP) inhibition, attenuation of neutrophil (PMN) activation, and elastase release. CMT-3's poor water solubility limits its bioavailability when administered orally for treating ALI. We developed a nano-formulation of CMT-3 (nCMT-3) to test the hypothesis that the pleiotropic anti-inflammatory activities of IT nCMT-3 can attenuate LPS-induced ALI. **Methods:** C57BL/6 mice were treated with aerosolized IT nCMT-3 or saline, then had IT LPS or saline administered 2 h later. Tissues were harvested at 24 h. The effects of LPS and nCMT-3 on ALI were assessed by lung histology, MMP level/activity (zymography), NLRP3 protein, and activated caspase-1 levels. Blood and bronchoalveolar lavage fluid (BALF) cell counts, PMN elastase, and soluble triggering receptor expressed on myelocytes-1 (sTREM-1) levels, TNF- α , IL-1 β , IL-6, IL-18, and BALF protein levels were also measured. **Results:** LPS-induced ALI was characterized by histologic lung injury (PMN infiltration, alveolar thickening, edema, and consolidation) elevated proMMP-2, -9 levels and activity, increased NLRP-3 protein and activated caspase-1 levels in lung tissue. LPS-induced increases in plasma and BALF levels of sTREM-1, TNF- α , IL-1 β , IL-6, IL-18, PMN elastase and BALF protein levels demonstrate significant lung/systemic inflammation and capillary leak. nCMT-3 significantly ameliorated all of these LPS-induced inflammatory markers to control levels, and decreased the incidence of ALI. **Conclusions:** Pre-treatment with nCMT3 significantly attenuates LPS-induced lung injury/inflammation by multiple mechanisms including: MMP activation, PMN elastase, sTREM-1 release, and NLRP3 inflammasome/caspase-1 activation.

KEYWORDS—ARDS, CMT-3, LPS, MMP, NLRP3 inflammasome and caspase-1, sTREM-1, tetracycline

INTRODUCTION

Acute respiratory distress syndrome (ARDS) is a life-threatening complication of sepsis with significant morbidity and mortality. In ARDS, an exaggerated inflammatory response to infection disrupts pulmonary capillaries causing alveolar flooding and pulmonary edema (1). The heterogeneous lung injury in ARDS results in stiff, noncompliant lungs which are difficult to ventilate and oxygenate. Current treatment of sepsis-related ARDS includes antibiotics to fight infection, fluid resuscitation, and vasopressors to maintain blood pressure, mechanical ventilation and dialysis for pulmonary, and renal support. Despite these treatments, the mortality rate from ARDS remains high (30%–40%). We believe this is due in part to the inability of current treatments to address the underlying role of systemic inflammation in the pathogenesis of the disease.

Chemically modified tetracycline 3 (6-demethyl-6-deoxy-4-dedimentylamino-tetracycline: CMT-3) is a nonantibacterial, anti-inflammatory agent with pleiotropic effects including: inhibition of MMP -2 and -9, neutrophil elastase and inflammatory cytokines (2, 3) as well as an increase in tissue inhibitor of metalloproteinase (TIMP)-1 (4). CMT-3 has been shown to attenuate sepsis-induced inflammation and lung injury in cecal-ligation puncture and porcine models of ARDS (4–6). Unfortunately, CMTs have only been available for oral administration due to poor solubility and high hydrophobicity that results in insufficient distribution to the disease site, thus limiting the anti-inflammatory effects in heterogeneous syndromes like ALI/ARDS. Nanomaterial-based delivery systems have been broadly applied in preclinical studies and clinical applications to increase bioavailability, reduce toxicity and improve pharmacokinetics via enhanced delivery (7, 8). Accordingly, CMT-3 has been formulated in lipid nanoparticles with particle sizes around 150 nm (9). Nanoparticles with smaller size are preferred to reduce the nonspecific clearance by the reticuloendothelial system and enhance tissue penetration (10).

The lung is an attractive route for noninvasive drug delivery, with many advantages, such as a high surface area with rapid absorption due to high vascularity and circumvention of the first pass effect. Aerosol drug delivery is commonly used to treat respiratory conditions (11) and is being actively

Address reprint requests to Juntao Luo, PhD, Department of Pharmacology and Surgery, SUNY Upstate Medical University, 750 E Adams St., Syracuse, NY 13210. E-mail: Luo@upstate.edu;

Co-correspondence: Robert N. Cooney, MD, Department of Surgery, SUNY Upstate Medical University, 750 E Adams St., Suite 8141, Syracuse, NY 13210. E-mail: cooneyr@upstate.edu

QM, XW, and DG contributed equally to this work.

The authors report no conflicts of interests.

Supplemental digital content is available for this article. Direct URL citation appears in the printed text and is provided in the HTML and PDF versions of this article on the journal's Web site (www.shockjournal.com).

DOI: 10.1097/SHK.0000000000001927

Copyright © 2022 by the Shock Society

investigated for systemic applications in multiple diseases (12). Nanoparticles expand the therapeutic potential of certain drugs as they can facilitate drug delivery via different routes, including inhalation (13). Telodendrimers are a novel linear-dendritic block copolymer with a well-defined dendritic domain for customized nanocarrier design for different therapeutic molecules (14, 15). In order to enhance the anti-inflammatory efficacy of CMT-3 in ARDS treatment and reduce lung injury, we developed a nano-formulation of CMT-3 (nCMT-3) using telodendrimers (15) that allows for targeted organ delivery and maximized therapeutic potential through aerosolization.

The current study tests the ability of prophylactic IT nCMT-3 to attenuate systemic inflammation and lung injury in an IT LPS murine model of ARDS. Our results provide evidence that IT nCMT-3 administration is effective in attenuating histologic lung injury and capillary leak (BALF protein levels) in this model. We also demonstrate that nCMT-3 inhibits multiple inflammatory pathways important in the pathogenesis of ARDS including the triggering receptor expressed on myeloid cells-1 (TREM-1) and NLRP3 inflammasome/caspase-1 pathways.

MATERIALS AND METHODS

Nanoparticle preparation and CMT-3 encapsulation

Following our previous publication (16), telodendrimer PEG^{5k}CA₄VE₄ was synthesized via a solution phase peptide chemistry as shown in Scheme S1 (see supplemental data 1, <http://links.lww.com/SHK/B431>) and described in supplementary information. Hydrophobic CMT-3 was encapsulated into a telodendrimer micelle using a thin film hydration method: Both CMT-3 and PEG^{5k}CA₄VE₄ at 1:20 mass ratio was dissolved in DCM and methanol (MeOH) (10:1 v/v) in a 10 mL round-bottom flask. A thin film was prepared by removing organic solvent on rotovaporation under vacuum and further dried under high vacuum. One milliliter of PBS buffer was then added to hydrate thin film followed by vortex and sonication. The particle size of CMT-3 encapsulated micelles was evaluated by DLS particle sizer. Nano-formulation solution was filtered with a 0.22 μm filter for sterilization. The drug loading efficiency was calculated to be ~100% by the drug concentrations before and after filtration. *In vitro* CMT-3 Release: 330 μL CMT-3-PEG^{5k}CA₄VE₄ nano-formulation was put into dialysis cartridges with a 3.5 kDa MWCO. The cartridges were dialyzed against 50 mL of PBS buffer at 37°C, and PBS buffer was refreshed every 4 h during the first 8 h and then every 12 h. The drug concentration remaining in the dialysis cartridge was measured at different time points by UV-vis spectrophotometry. The release profile was presented as a mean of triplicates with standard deviations.

Cell viability assay

Murine macrophage cell RAW 264.7, human monocyte THP-1 cells and human alveolar basal epithelial cell A549 were purchased from American Type Culture Collection (ATCC, USA) and were cultured in DMEM or RPMI-1640 with 10% fetal bovine serum (FBS), 100 μg/mL streptomycin and 100 U/mL penicillin G at 5% CO₂, 37°C in a humidified incubator. Mouse alveolar macrophages (AM) were isolated from pulmonary alveoli by washing the lung using bronchoalveolar lavage (BAL) as previously described (17). Cells were seeded in 96-well plates at a density of 6,000 cells/well. After overnight incubation, free CMT-3 (in DMSO), CMT-3-PEG^{5k}CA₄VE₄, and blank PEG^{5k}CA₄VE₄ with different concentrations were added into each well and incubated for 48 and 72 h, respectively. CellTiter 96[®] Aqueous Cell Proliferation Reagent composed of MTS and PMS reagents was added into each well according to the manufacturer's instructions and further incubated at 37°C for 2 h in RAW 264.7 and 4 h in THP-1 cells. The cell viability was measured by UV-absorbance at 490 nm in a microplate reader (BioTek Synergy H1). The untreated cells are considered as control. Results were calculated from the equation cell viability % = (OD treat-OD blank) / (OD control-OD blank) × 100% (n = 3).

Pharmacokinetic and tissue biodistribution

1. Animals and treatment:

Healthy C57BL/6J mice aged 6 to 8 weeks had a single dose of nCMT-3 administered by an intratracheal (IT, 2 mg/kg, n = 3) or intravenous (IV, 1 mg/kg, n = 2) route. Mice were euthanized at 10 min, 15 min, 30 min, 2 h,

4 h, 8 h, and 24 h and blood, heart, kidney, liver, lung, and spleen were harvested. The organs were washed with PBS and homogenized with extraction buffer (10% Triton X-100, deionized water, and acidified iso-propanol (0.75 N HCl) at 1:2:15 v/v/v) by tissue grinder.

2. Standard samples of plasma and tissues.

Plasma from healthy mice was collected and stored at -80°C. To construct a calibration curve, different volumes of CMT-3 were added to 50 μL of plasma with 150 μL PBS to obtain CMT-3 standard concentrations ranging from 0.5 to 50 μg/mL in plasma. Fifty milligrams of tissues (from heart, kidney, liver, lung, and spleen) were homogenized with 2-fold weight of PBS and 5-fold weight of extraction buffer. Three hundred fifty microliters aliquots of homogenates were spiked with CMT-3 solutions to prepare homogenates with CMT-3 concentrations ranging from 0.5 to 50 μg/mL.

3. Solid phase extraction:

Two hundred microliters of plasma was acidified using 8 μL of 50% phosphoric acid and vortex-mixed for 30 s. Tissue homogenates: heart, kidney, liver, lung, and spleen tissues were homogenized with 7-fold weight of extraction buffer and incubated at -20°C overnight. The homogenate and plasma samples were spun down and the supernatant was transferred onto C18 extraction cartridge (Waters Corporation, Milford, MA) that was conditioned and equilibrated by washing with 1 mL of methanol (100, v/v) and 1 mL of Milli-Q water. The cartridge was washed with 0.5 mL of methanol/water (5/95, v/v). Analytes were eluted with 2 mL of methanol (100, v/v). After evaporation, the samples were reconstituted with 125 μL acetonitrile. Seventy microliters of acetonitrile extraction solution was taken and mixed with 30 μL water for high-performance liquid chromatography (HPLC) analysis.

Animals and lung injury model

Male and female C57BL/6 mice (age: 8 weeks) were purchased from Jackson Laboratories (Bar Harbor, ME). All animals were housed under controlled temperature (22°C) and photoperiod (12-h light and 12-h dark cycle) with free access to water and food. The animal experiments were approved by the Institutional Animal Care and Use Committee of the SUNY Upstate Medical University (IACUC # 344). All studies were performed in accordance with the National Institutes of Health and ARRIVE guidelines on the use of laboratory animals. The dose of IT LPS used in this study was not associated with mortality in any of the experimental groups.

Acute lung injury induction, nCMT-3 treatment and tissue harvest

All mice underwent noninvasive tracheal installation by aerosolizer with nCMT-3 (1 mg/kg) or vehicle 2 h before induction of lung injury by LPS (2.5 mg/kg) or saline as described previously (18). Briefly, the mice in the septic and control groups were anesthetized by intraperitoneal injection with a combination of ketamine (80 mg/kg) and xylazine (8 mg/kg). After the induction of anesthesia, mice were suspended by their incisors in the supine position on the intubating platform and the fiber-optic illuminator was positioned over the trachea. Forceps were used to carefully retract the tongue and in an upward and leftward position to gain visualization of the larynx. Hands-free binocular magnifiers were used to improve visualization of the larynx. MicroSprayer Aerosolizer (Cat. #: YAN30012, Shanghai Yuyan Instruments Co., Ltd) was inserted into the tracheal lumen and LPS, nCMT-3 and saline solution (volume not to exceed 70 μL per mouse) were instilled. The mouse was maintained in the same position on the intubating platform for at least 30 s, and then placed prone on a heating pad for recovery. All surviving mice were sacrificed under anesthesia at 24 h post-LPS, then frozen (in EDTA), lung tissue (fixed with 10% formalin lung histology and broden for protein analysis) and bronchoalveolar lavage fluid (BALF) were collected.

Cytological analysis in BALF

BALF was obtained from mouse lung and lavaged with 3 × 0.5 mL of sterile saline, and then centrifuged at 250 × g for 10 min. The pellet was resuspended with 1 mL of sterile saline. One hundred microliters of cell suspension were centrifuged by Cytospin centrifuge (Hettich ROTOFIX 32A) at 1,000 rpm for 3 min to mount the cells on a slide. The slide was air-dried and stained with Hema-3 (Fisher Scientific, Kalamazoo, MI) for analysis. Neutrophils and macrophages were counted 20 high power fields (HPF) by blinded reviewers using Nikon Eclipse TE2000-U research microscope (Nikon, Melville, NY).

Western blot and ELISA

Frozen lung was homogenized in RIPA buffer and extracted protein was used for Western blot analysis. Total protein concentrations from lung and BALF

were determined by the BCA micro assay kit (Thermo Scientific, Rockford, IL). Twenty microliters of protein were separated by SDS-PAGE gel, then transferred to PVDF membranes (Millipore Co., Ltd., USA). The membranes were incubated with 5% nonfat milk (Bio-Rad Laboratories) in Tris-buffered saline plus 0.5% Tween-20 (TBS-T) for 1 h at room temperature, and then overnight at 4°C with primary antibodies purchased from Santa Cruz Biotechnology, including caspase-1 (Cat. #: sc-56036, 1:200 dilution) and NLRP3 inflammasome (Cat. #: sc-134306, 1:200 dilution). The secondary antibody linked to horseradish peroxidase (HRP) purchased from Santa Cruz Biotechnology (Cat. #: 1662408, Bio-Rad Laboratories) was applied for 1 h at room temperature. Antibody-antigen complexes were visualized using ECL according to the manufacturer's instructions. The images were analyzed quantitatively by densitometry with Image J software. The relative density of immunoreactive bands was normalized to the density of the corresponding GAPDH bands.

Blood sample and BALF were collected for the measurements of TNF- α , (Cat. #: 50-112-8800, Invitrogen), IL-1 β (Cat. #: 50-112-8814, Invitrogen), IL-6 (Cat. #: 50-112-8863, Invitrogen), neutrophil elastase (Cat. #: ab252356, Abcam), soluble TREM-1 (Cat. #: EMTREM1, Thermo Fisher Scientific Inc.), and IL-18 (Cat. #: BMS618-3, Invitrogen). All cytokines were measured using commercial ELISA kits according to the manufacturer's instructions.

Histological assessment of lung injury

Lungs were inflation-fixed for histology by tracheal instillation of 0.5 mL of 10% neutral formalin. Fixed lungs were embedded in paraffin. Five micrometers sections of lung tissues were stained with Hematoxylin and Eosin (H&E). Histopathology was evaluated in a blinded manner by two independent pathologists. The histopathological assessment of acute lung injury was performed using a 0–2 scoring system described in a previous study (19). Briefly, neutrophils in the alveolar space and in the interstitial space were counted separately. Hyaline membranes, proteinaceous debris filling the airspaces and septal thickening were evaluated. To generate a lung injury score, the sum of each of the five independent parameters weighted according to the relevance ascribed to each feature was taken and then were normalized to the number of fields evaluated. Three representative fields per slide were counted in 20 high power fields (HPF) by blinded reviewers at $\times 400$ magnification under light microscopy.

Gelatin zymography

Gelatin zymography was used to quantify MMP-2 and MMP-9 activity in lung tissues. Ten micrograms of total protein were subject to electrophoresis on sodium dodecyl sulfate-polyacrylamide gel electrophoresis gels that contained 0.1% gelatin as a substrate for MMP digestion. After electrophoresis, the gels were incubated for 24 h, then stained with Coomassie Blue, and MMP activity was assessed by quantifying cleared bands of substrate lysis. The MMPs were identified by their molecular weights and inhibition by ethylenediaminetetraacetic acid or phenanthroline. Activity was quantified by scanning densitometric analysis using with NIH Image J software.

Statistical analysis

The data are expressed as mean \pm SEM. Statistical analysis of the data was performed using GraphPad Prism software (version 5.0). The sample size for each experimental group ($n=x$) is presented in the figure legend. One-way analysis of variance (one-way ANOVA) with Bonferroni's multiple comparisons test was used to determine group differences. Differences among groups were considered significant at $P < 0.05$. All data was obtained from three or more independent experiments.

RESULTS

Preparation and characterization of nCMT-3 using telodendrimer (PEG^{5k}CA₄VE₄)

Following our procedure (16), we synthesized a hybrid telodendrimer using cholic acid (CA) and vitamin E (VE) as peripheral groups to increase drug binding as well as increase micelle stability by the amphiphilic CA. As shown in sFigure 2A (supplemental data 2, <http://links.lww.com/SHK/B432>), CMT-3 was successfully encapsulated by PEG^{5k}CA₄VE₄ nanocarrier at a 1:20 mass ratio with homogeneous particle size at 27 nm with 100% drug loading efficiency. The small particle size of the nanoformulation allows convenient

administration of CMT-3-PEG^{5k}CA₄VE₄ through IV or IT injection and facilitates pulmonary deposition and tissue penetration. TEM images shown in sFigure 2B reveal the spherical particle morphology for the blank PEG^{5k}CA₄VE₄ and CMT-3 loaded PEG^{5k}CA₄VE₄ nanoparticles. As shown in sFigure 2C, the nanocarrier sustained CMT-3 release for 24 h with an initial phase of fast drug release of 50% within 4 h, enabling immediate drug action. CMT-3 is barely soluble in aqueous solutions, which prevents side-by-side comparison with nCMT-3 in drug release. sFigure 2D shows the blank PEG^{5k}CA₄VE₄ telodendrimer is nontoxic up to 1 mg/mL for immune cells (RAW 264.7 and THP-1) in cell culture. In contrast, free CMT-3 and nCMT-3 levels from 10³ to 10⁴ ng/ml have no effect on Raw 264 cell viability, whereas concentrations in the 10² to 10³ ng/ml range reduce THP-1 cell viability. IT administration of nCMT-3 in our study results in plasma/tissue levels from 1,800 to 80 ng/mL over 24 h (Fig. 1) which should have minimal effects on cell viability. To further determine if nCMT-3 was toxic to immune cells or lung tissue we examined the effects of nCMT-3 on viability of alveolar epithelial cells (A549 cells) and primary murine alveolar macrophages from LPS-treated mice (sFig 5). In these studies, nCMT-3 concentrations <2500 ng/mL had minimal effects on cell viability. Based on these studies, we do not believe the anti-inflammatory effects of nCMT-3 are due to immune cell toxicity.

Pharmacokinetics and biodistribution of nano-CMT-3 formulations

The pharmacokinetic profiles and biodistribution of nCMT-3 were investigated in C57BL/6J mice after IV or IT administration. As shown in Figure 1A, nCMT-3 concentrations decrease over time after IV administration. In contrast, plasma concentrations of nCMT-3 peaked at 30 min after IT dosing and decreased more slowly over time compared to IV administration. This finding suggests nCMT-3 continues to diffuse into the blood stream from lung tissue after IT administration. The concentration of CMT-3 in lung tissue was significantly higher and was sustained for up to 8 h in mice following IT administration of nCMT-3 compared with those treated with IV injection (Fig. 1B). By comparison, intravenous injection of nCMT-3 led to relatively undetectable levels of nCMT-3 in the lung. The drug concentrations in the liver and kidney (Fig. 1C and D) were also significantly higher in the IT-treated animals, likely due to the lung acting as a drug depot and providing continuous drug release, which may effectively protect these remote organs from hyperinflammatory damage in sepsis. Preliminary data (not shown) suggests IT nCMT-3 attenuates acute kidney injury in the IT LPS model, additional studies will be needed to characterize the effects of nCMT-3 on hepatocellular function.

Matrix metalloproteinase activity and neutrophil elastase levels in LPS-induced ALI

The induction and activation of MMPs and neutrophil elastase are common mechanisms of lung injury in ARDS. Therefore, we examined the ability of IT nCMT-3 to regulate their abundance and activity in LPS-induced ARDS. CMT-3 is an MMP inhibitor and can reduce MMP-2 and -9 activity and neutrophil elastase levels in lung injury. Gelatin zymography

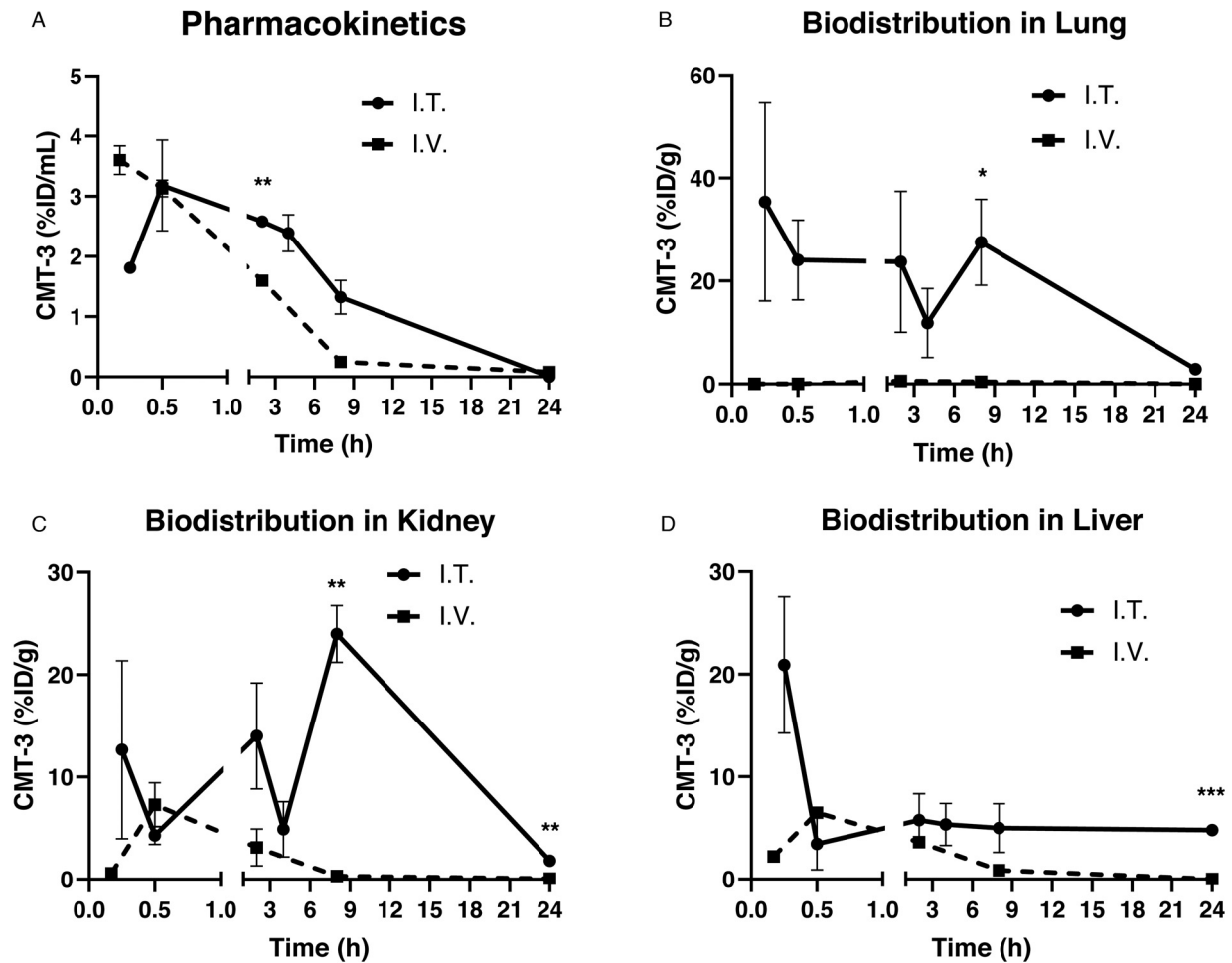


FIG. 1. Pharmacokinetics and biodistribution of nCMT-3 after IV or IT administration. CMT-3 concentration in plasma (A) and major organs lungs (B), kidney (C) and liver (D) as calculated as percentage of administered dose as analyzed by HPLC after solid-phase extraction. HPLC indicates high-performance liquid chromatography; IV, intravenous injection; IT, intratracheal injection; nCMT-3, nano-formulation of chemically modified tetracycline 3.

was used to measure MMP levels and activity in lung tissue (Fig. 2). The LPS-induced increase in lung MMP-2 and -9 were detected by gelatin zymography (Fig. 2A), showing that treatment with nCMT-3 significantly reduced pro-MMP-9 (Fig. 2B), active MMP-9 (Fig. 2C), and active MMP-2 (Fig. 2D) were significantly attenuated by prophylactic nCMT-3 administration (LPS vs. LPS/nCMT-3, $P < 0.05$). Pre-treatment with nCMT-3 also blocked the LPS-induced increase in plasma (Fig. 2E) and BALF (Fig. 2F) neutrophil elastase levels (LPS vs. LPS/nCMT-3, $P < 0.05$). These results provide evidence that IT administration of nCMT-3 inhibits MMP induction, activation and increased neutrophil elastase levels in LPS-induced ALI.

Analysis of lung histology and bronchoalveolar lavage fluid (BALF) in LPS-induced ALI

Lung histology was assessed to evaluate the ability of nCMT-3 to attenuate LPS-induced lung injury (Fig. 3). Histologic lung injury was characterized by PMN infiltration, alveolar hemorrhage and edema, as well as hyaline membrane formation as described in Methods. Pretreatment with nCMT-3 attenuated both histologic lung injury (Fig. 3A) and the lung injury score

(Fig. 3B) in LPS-induced lung injury (LPS vs. LPS/nCMT-3, $P < 0.05$).

Analysis of BALF is commonly used to assess lung injury, inflammation and severity in experimental ARDS. Normally, BALF contains fewer than 100 WBC/ μ L which are predominately macrophages with few neutrophils, lymphocytes or eosinophils. As shown in Figure 4, LPS-induced lung injury is associated with a marked increase in BALF white blood cells, especially neutrophils (Fig. 4B) and macrophages (Fig. 4C) which were attenuated by pretreatment with nCMT-3 (LPS vs. LPS/nCMT-3, $P < 0.05$). BALF protein was measured as an indicator of alveolar-capillary membrane permeability. As shown in Figure 4D, the increase in BALF protein by LPS was attenuated by nCMT-3 administration ($P < 0.05$ LPS vs. Vehicle and LPS/nCMT-3). These findings provide evidence that nCMT-3 attenuates pulmonary edema in LPS-induced lung injury.

Inflammatory cytokines are produced during acute lung injury and can upregulate the host response to infection by activating immune cells. Levels of proinflammatory cytokines in BALF and plasma are frequently measured to assess pulmonary and systemic inflammation in experimental ARDS. Given

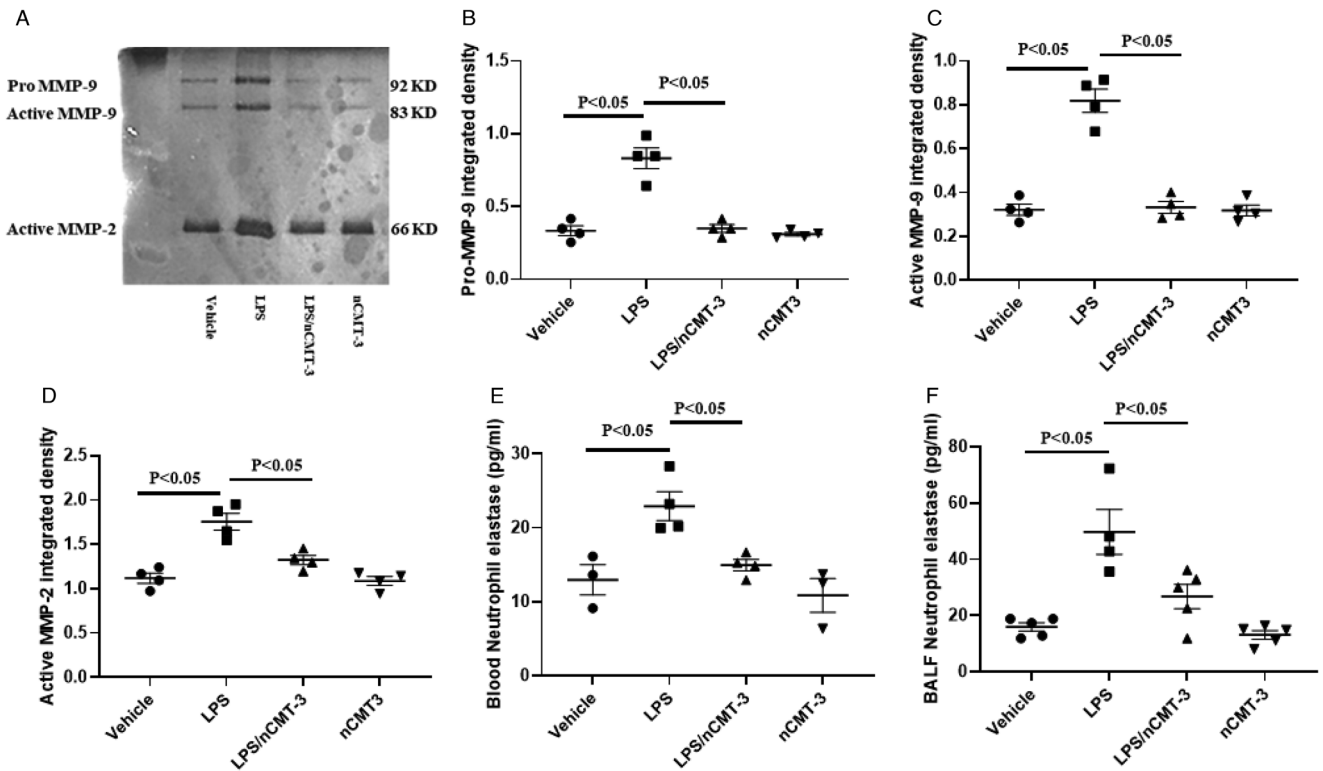


FIG. 2. Matrix metalloproteinase activity and neutrophil elastase levels in LPS-induced lung injury. Mice were treated with nano-CMT-3 (1 mg/kg) or vehicle 2 h before induction of lung injury by LPS (2.5 mg/kg) or sham lung injury (by saline) using non-invasive tracheal installation by aerosolizer. Mice were sacrificed 24 h after LPS or saline, then lung tissue was collected for protein isolation. Gelatin zymography was used to detect MMP-2 and MMP-9. Plasma and BALF were collected for NE by ELISA. Representative gelatin zymography showed the differences in pro MMP-9/active MMP-9 and active MMP-2 in panel A. The abundances of pro MMP-9 (B), active MMP-9 (C) and active MMP-2 (D) were quantified using Image J. The levels of NE in plasma (E) and BALF (F) were assayed. Scatter dot plot represents mean values and standard error of mean (SE) (n = 4/group). BALF indicates bronchoalveolar lavage fluid; CMT-3, chemically modified tetracycline 3; LPS, lipopolysaccharide; MMP, matrix metalloproteinase; SE, standard error.

this, we examined the effects of LPS and nCMT-3 on plasma and BALF levels of TNF- α , IL-1 β , IL-6, and IL-18 in our LPS lung injury model (Fig. 5). Plasma cytokine levels of TNF α , IL-1 β , and IL-6 were not significantly different in the LPS and

LPS/nCMT-3 groups at 24 h (data not shown). In contrast, nCMT-3 significantly attenuated the LPS-induced increase in TNF- α (Fig. 5A), IL-1 β (Fig. 5B), IL-6 (Fig. 5C), and IL-18 (Fig. 5D) in BALF and IL-18 (Fig. 5E) in plasma (LPS vs. LPS/

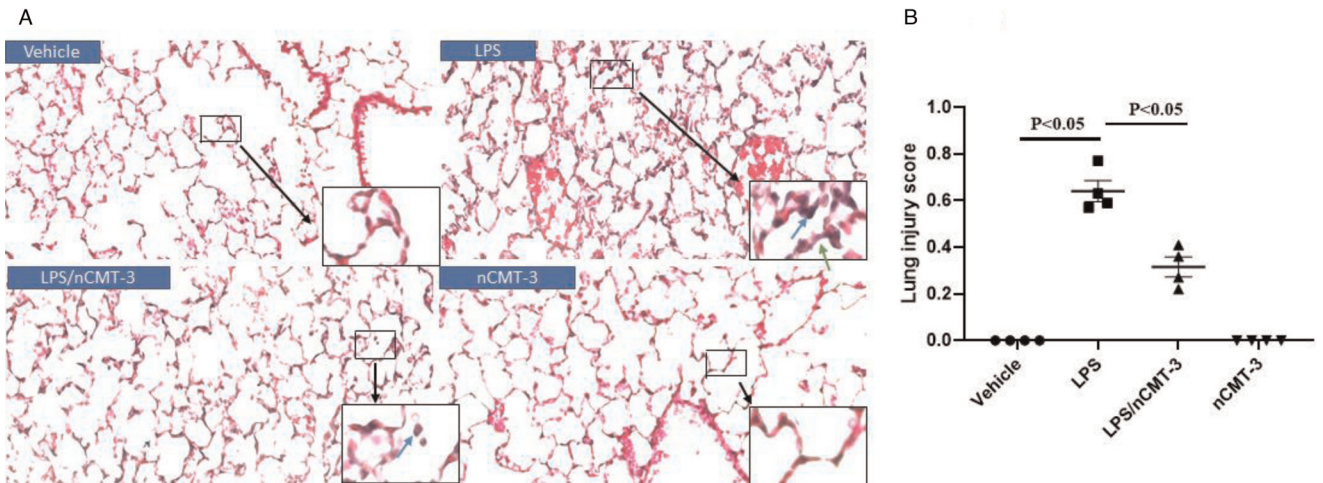


FIG. 3. Histological assessment of lung injury: Mice were treated with nano-CMT-3 (1 mg/kg) or vehicle 2 h before induction of lung injury by LPS (2.5 mg/kg) or sham lung injury (by saline) using noninvasive tracheal installation by aerosolizer. Mice were sacrificed 24 h after LPS or saline, then lung tissue was collected for H&E staining to evaluate lung injury from each group (A). Lung injury was characterized by neutrophil infiltration (blue arrows), hyaline membranes, proteinaceous debris filling the airspaces and alveolar septal thickening (green arrow). Semi-quantitative histological lung injury score was assessed (B). Scatter dot plot represents mean values and standard error of mean (SE) (n = 4–5/group). CMT-3 indicates chemically modified tetracycline 3; LPS, lipopolysaccharide; SE, standard error.

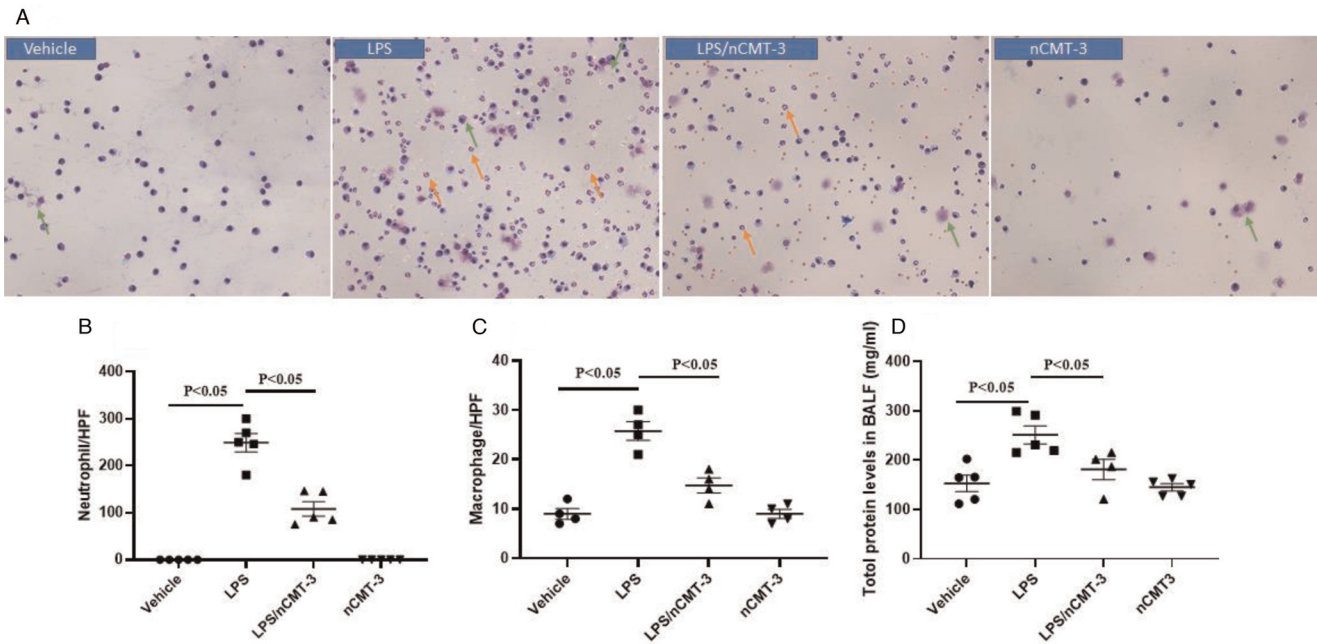


FIG. 4. Cytological analysis and total protein concentration in bronchoalveolar lavage fluid (BALF): Mice were treated with Nano-CMT-3 (1 mg/kg) or vehicle 2 h before induction of lung injury by LPS (2.5 mg/kg) or sham lung injury (by saline) using noninvasive tracheal installation by aerosolizer. Mice were sacrificed 24 h after LPS or saline, then BALF was collected for examining neutrophils (orange arrows) and macrophages (green arrows) by Hema 3 staining (A). Quantification of neutrophils (B) and macrophages (C) per slide were counted at $\times 400$ magnification under light microscopy. Total protein concentration was assayed by BCA (D). Scatter dot plot represents mean values and standard error of mean (SE) ($n = 4-5$ /group). BALF indicates bronchoalveolar lavage fluid; CMT-3, chemically modified tetracycline 3; LPS, lipopolysaccharide.

nCMT-3, $P < 0.05$). These results provide evidence that prophylactic administration of IT nCMT-3 significantly attenuates lung injury/inflammation as well as systemic inflammation in the LPS-induced lung injury model.

TREM-1 and NLRP3 inflammasome/caspase-1 pathways in LPS-induced ALI

TREM-1 is a triggering receptor expressed on neutrophils and monocytes which plays an important role in amplifying inflammation during systemic infection and other conditions. Recent studies suggest that crosstalk and synergistic activation of the TREM-1 and NLRP3 inflammasome/caspase-1 pathways represent an important mechanism of lung injury and inflammation in ARDS. To assess the effects of LPS and nCMT-3 on the TREM-1 pathway, we measured soluble TREM-1 (sTREM-1) levels in plasma and BALF (Fig. 6). sTREM-1 levels were increased in plasma (Fig. 6A) and BALF (Fig. 6B) by LPS ($P < 0.05$ vs. Vehicle) and restored to control levels in the LPS/nCMT-3 group ($P < 0.05$ vs. LPS). Next, we examined the relative abundance of NLRP3 inflammasome and caspase-1 in lung tissue by Western blot as shown in Figure 7. The elevations in NLRP3 inflammasome (Fig. 7A) and caspase-1 (Fig. 7B) in LPS-induced lung injury were ameliorated by prophylactic nCMT-3 administration. Consistent with this observation, the increased levels of IL-1 β and IL-18 observed in BALF (Fig. 5B and D) from LPS-treated mice were ameliorated by nCMT-3 administration. Collectively these data suggest prophylactic IT nCMT-3 attenuates LPS-induced inflammation by regulating the TREM-1 and NLRP3 inflammasome/caspase-1 inflammatory pathways.

Effect of telodendrimer (PEG^{5K}CA₄VE₄) alone on ALI induced by LPS in mice

To accurately estimate the effect of nCMT-3 on lung injury from CMT-3 rather than telodendrimer (PEG^{5K}CA₄VE₄) (Nano), we designed a new experiment involving the use of Nano in lung injury group. We counted leukocytes (neutrophil to lymphocyte ratio, NLR [%]) and examined proinflammatory IL-6 and neutrophil/macrophage levels in BALF. We found that pre-treatment of Nano had no significant attenuation on increased blood NLR (%), IL-6 (see supplemental data 3, sFig. 3, <http://links.lww.com/SHK/B433>) and neutrophil/macrophage in BALF (see supplemental data 4, sFig. 4, <http://links.lww.com/SHK/B434>), suggesting that the improvement of lung injury by using nCMT-3 was mainly due to the pharmacological effect of CMT-3 in our current study.

DISCUSSION

Despite decades of research, the current options for treating ARDS are limited and have done little to reduce the morbidity and mortality of the disease. Contemporary management of ARDS includes treating the underlying cause (e.g., sepsis and gastric aspiration), protective mechanical ventilation to prevent ventilator-induced lung injury and supportive critical care (e.g., resuscitation, vasopressors, and renal replacement therapy). The current study has several important findings that are novel and may help us develop effective strategies to treat the severe systemic inflammation that contributes to lung injury in ARDS. First, intratracheal delivery of nanoformulated CMT-3 results in enhanced levels of nCMT-3 in lung

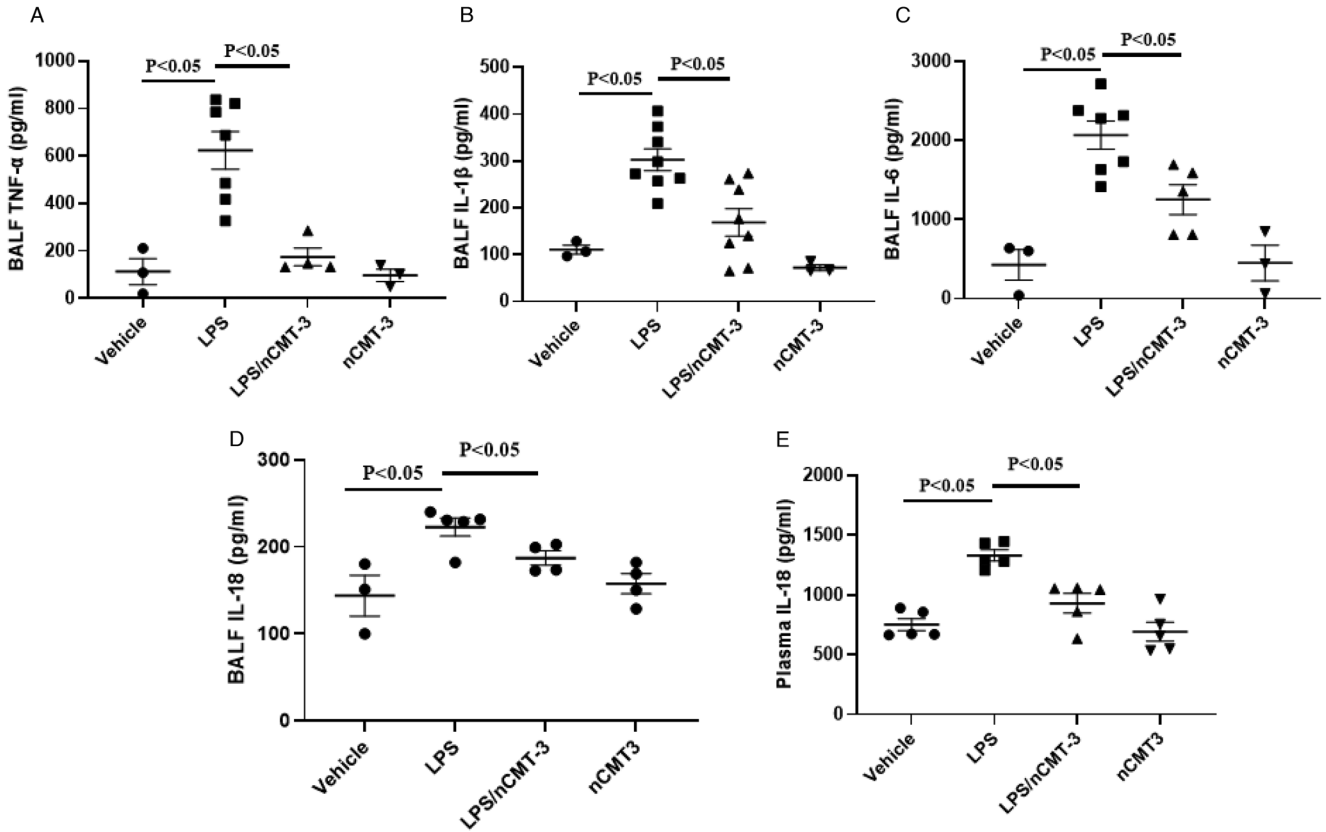


FIG. 5. Cytokine levels in bronchoalveolar lavage fluid (BALF) and plasma: Mice were treated with nano-CMT-3 (1 mg/kg) or vehicle 2 h before induction of lung injury by LPS (2.5 mg/kg) or sham lung injury (by saline) using non-invasive tracheal installation by aerosolizer. Mice were sacrificed 24 h after LPS or saline, then BALF and plasma were collected for cytokines by ELISA. TNF- α (A), IL-1 β (B), IL-6 (C), and IL-18 (D) in BALF and IL-18 (E) in plasma were assayed. Scatter dot plot represents mean values and standard error of mean (SE) (n = 3–12/group). BALF indicates bronchoalveolar lavage fluid; CMT-3, chemically modified tetracycline 3; LPS, lipopolysaccharide; SE, standard error.

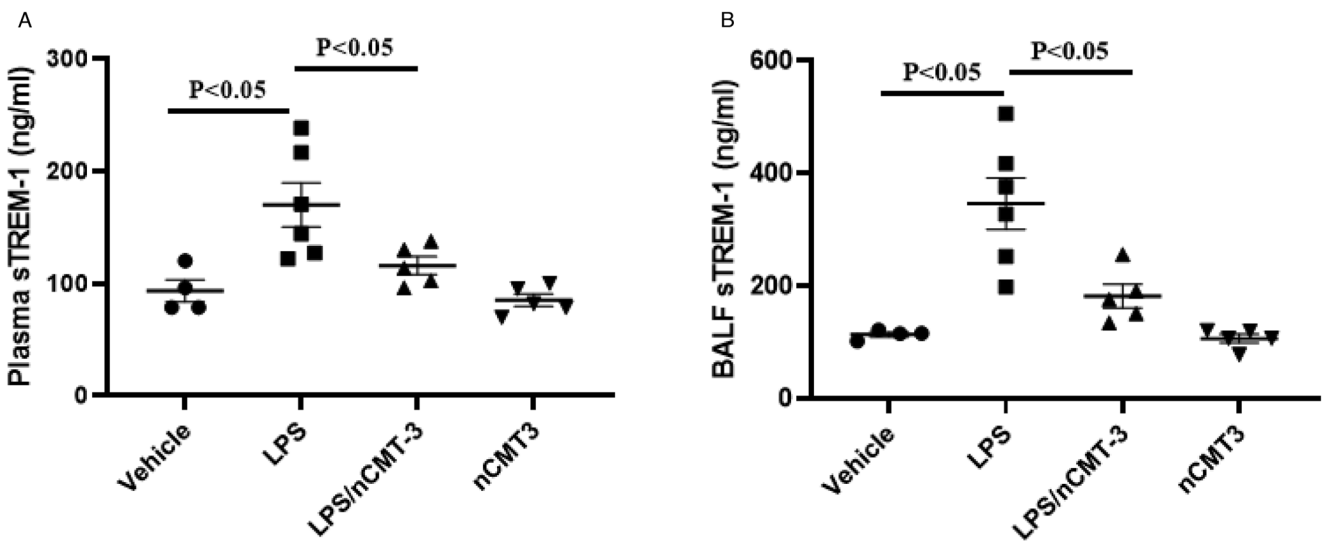


FIG. 6. The levels of soluble triggering receptor expressed on myeloid cells 1 (sTREM-1) in blood and BALF: Mice were treated with Nano-CMT-3 (1 mg/kg) or vehicle 2 h before induction of lung injury by LPS (2.5 mg/kg) or sham lung injury (by saline) using non-invasive tracheal installation by aerosolizer. Mice were sacrificed 24 h after LPS or saline, then plasma and BALF were collected for NE and sTREM-1 by ELISA. Plasma sTREM-1 (A) and BALF sTREM-1 (B) were assayed. Scatter dot plot represents mean values and standard error of mean (SE) (n = 3–5/group). BALF indicates bronchoalveolar lavage fluid; CMT-3, chemically modified tetracycline 3; LPS, lipopolysaccharide; SE, standard error; sTREM-1, soluble triggering receptor expressed on myelocytes-1.

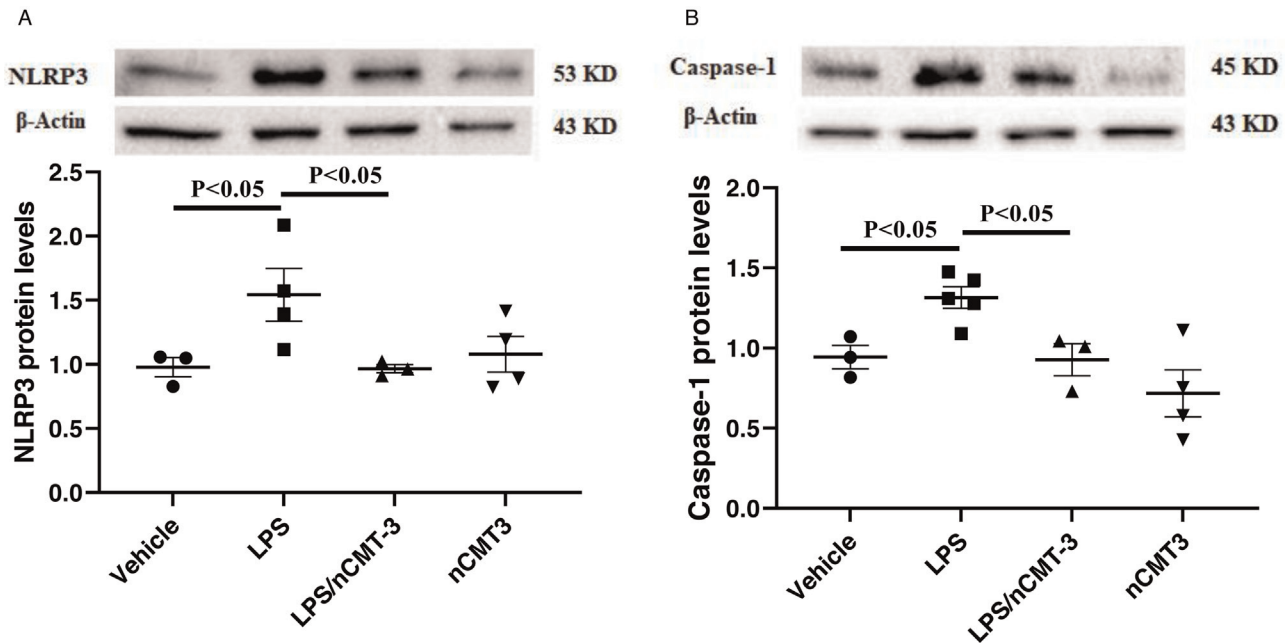


FIG. 7. The levels of caspase-1 and NPRL3 inflammasome in lung tissue: Mice were treated with nano-CMT-3 (1 mg/kg) or vehicle 2 h before induction of lung injury by LPS (2.5 mg/kg) or sham lung injury (by saline) using non-invasive tracheal installation by aerosolizer. Mice were sacrificed 24 h after LPS or saline, then lung tissues were harvested for protein analysis. Caspase-1 (A) and NPRL3 (B) inflammasome were measured by Western Blot. Scatter dot plot represents mean values and standard error of mean (SE) ($n=3-5/$ group). CMT-3 indicates chemically modified tetracycline 3; LPS, lipopolysaccharide; SE, standard error.

tissue compared with intravenous administration. Second, prophylactic nCMT-3 significantly attenuates multiple synergistic inflammatory pathways causing lung injury in experimental ARDS including: the matrix metalloproteinase and neutrophil elastase pathways, the NLRP3 inflammasome-caspase-1 pathway, the TREM-1 pathway and IL-1/IL-18 inflammatory cytokine pathways. Although IT nCMT-3 did not alter plasma TNF, IL-1, or IL-6 levels in this model, it significantly reduced multiple inflammatory pathways in experimental ARDS which are important in human ARDS. Our findings provide evidence that aerosolized nCMT-3 is effective in attenuating lung injury in ARDS and provides new insights regarding the multiple inflammatory pathways by which nCMT-3 acts.

Several studies have shown that tetracyclines like CMT-3 can attenuate lung injury and reduce mortality in experimental models of ARDS (4–6, 20–26). They also provide evidence that the inhibitory effects of tetracyclines on MMP 2 and 9 represent an important mechanism for reducing the infiltration of inflammatory cells and inflammatory mediator production in experimental models of ARDS (6, 21–23, 25). Consistent with previous studies examining the effects of oral CMT-3 on lung injury, we show that aerosolized nCMT-3 attenuates MMP 2 and 9 activities, levels of neutrophil elastase, BALF inflammatory cytokines (TNF- α , IL-1 β , IL-6, and IL-18), the amount of protein and numbers of neutrophil/macrophage in BALF, and histological lung injury score in a murine model of ARDS.

In addition to inhibiting MMPs, CMT-3 has pleiotropic anti-inflammatory properties. Up-to-date, the signaling pathway/molecular targets by which CMT-3 alleviates lung injury have not been completely elucidated, although some studies have been conducted. Since Weiss et al. identified a MMP-9

cleavage site in TREM-1 (27), we explored TREM-1 as a possible target of CMT-3. TREM-1 is an immunoglobulin cell surface receptor which is expressed on white blood cells and amplifies Toll-like receptor (TLR)-mediated inflammation during infection. Blocking TREM-1 activation has been shown to improve survival and attenuate the inflammatory response in sepsis (28, 29) because TREM-1 amplifies inflammation by regulating NF- κ B and TLR-ligands (28, 30). The effect of tetracycline and CMT-3 in inhibiting NF- κ B signaling has also been investigated in LPS-stimulated injury models (31). TREM-1 expression has been found on the surfaces of neutrophils, mature monocytes, macrophages and nonmyeloid cells, such as epithelial and endothelial cells (32). The extracellular domain can be detected in body fluids as soluble TREM-1 (sTREM-1). Although sTREM-1 has been proposed to act as an endogenous decoy receptor and binds TREM-1 ligands, the levels of circulating sTREM-1 have been shown to reflect TREM-1 activation and are a reliable biomarker in patients with septic shock (33). The reductions in plasma and BALF sTREM-1 levels observed in nCMT-3 treated mice provide evidence that nCMT-3 attenuates LPS-induced lung injury by preventing TREM-1 activation. Synergistic interactions between the TREM-1 and the NLRP3 inflammasome pathways contribute to rapid amplification of inflammatory stimuli in severe sepsis (34). Therefore, we characterized the effects of nCMT-3 on this pathway as well.

Activation of the NLRP3/Caspase-1 pathway is a major contributor in the development of ARDS (35, 36). NLRP3 inflammasomes are key to host immune defense against bacterial, fungal, and viral infections. NLRP3 inflammasomes mainly exist in immune and inflammatory cells (e.g., macrophages, monocytes, dendritic cells, and splenic neutrophils)

and are activated by inflammatory stimulation. Activation of the NLRP3 inflammasome by PAMPs or DAMPs (e.g., LPS) via TLRs-NF- κ B signaling increases active NLRP3, pro-IL-1 β , pro-IL-18, and the subsequent assembly of NLRP3, ASC (apoptosis-associated speck like protein containing a caspase recruitment domain), and procaspase-1 into a complex which triggers the conversion of procaspase-1 to caspase-1, as well as secretion of mature IL-1 β and IL-18. We believe the effects of nCMT-3 on the NLRP3/caspase-1 pathway explains why circulating IL-18 and BALF levels of IL-1 and IL-18 levels were impacted by nCMT-3.

The success of tetracycline in treating patients with ARDS by inhibiting caspase-1 activation directly (not including NLRP3 activation) (37) led us to hypothesize that CMT-3 might have a similar effect on lung injury. Tetracycline reduces high IL-1 β and IL-18 levels in the patients with direct ARDS *ex vivo*. (37). Additionally, CMT-3 significantly suppressed IL-1 β production in alveolar leukocytes isolated from patients within 24 h of the onset of direct ARDS (37). Therefore, this group postulates that tetracycline as an immunomodulatory drug is worthy of clinical evaluation for patients with direct ARDS. Although high levels of nCMT-3 (10^3) impact cell viability in cultured monocytes, tissue levels of nCMT-3 are lower than this and nCMT-3 was not cytotoxic to murine alveolar macrophages or cultured alveolar epithelial cells at plasma/tissue concentrations seen in this study. Thus, cytotoxic effects on immune cells do not appear to be the predominant mechanism for the anti-inflammatory effects of nCMT-3 in this study (see supplemental data 5, <http://links.lww.com/SHK/B435>).

On the basis of their observations, we utilized our direct lung injury by LPS in murine models to examine the levels of NLRP3, caspase-1 and proinflammatory cytokines (IL-1 β and IL-18). Our findings indicating that CMT-3 decreases the elevated levels of NLRP3 and caspase-1 induced by LPS in lung tissues, as well as IL-1 β in BALF and IL-18 in plasma and BALF. Our findings have revealed that both of NLRP3 and caspase-1 are reduced by nCMT-3. A study using the tetracycline derivative minocycline by Lu et al. in ischemia-induced brain damage reports similar results to our findings (38). The activation of NLRP3 inflammasome triggers caspase-1 activation and IL-1 β /IL-18 secretion, eventually resulting in an inflammatory and pyroptotic cell death. Our group plans to investigate the NLRP3/caspase-1 pathways to identify the precise target of CMT-3.

Previous studies have shown that TREM-1 activation increases LPS-induced IL-1 β in human monocytes via activation of the NLRP3 inflammasome and that TREM-1 aggravates inflammation in ALI by activating NLRP3 inflammasome with the involvement of NF- κ B activation (39). Another study has demonstrated that conditioned media from NLRP3 inflammasome-activated macrophages increases TREM-1 expression by HMGB1 and IL-18 through the activation of ROS-NF- κ B signals (34). In addition, inhibition of NLRP3 inflammasome reduces lung injury and TREM-1 expression in mice (34). This evidence suggests that the effect of CMT-3 on TREM-1 reduction is not only through direct inhibition of MMP-9, but also via indirect effect on NLRP3/NF- κ B activation.

Our studies provide evidence that prophylactic IT administration of nCMT-3 can attenuate LPS-induced lung injury. The mechanisms for this appear to be multifactorial and potentially include reductions in TREM-1 and NLRP3 inflammasome/caspase-1 signals. Increases in MMP 2 and 9, neutrophil elastase and proinflammatory cytokines can be attenuated by free CMT-3 in lung injury. Consistent with these mechanisms, increases in the above markers we observed in LPS-induced lung injury were ameliorated by nCMT-3. The key finding in our study was that nCMT-3 attenuated the increase in TREM-1 and deactivated NLRP3/caspase-1 signals. Collectively these data provide evidence that nCMT-3 can attenuate lung injury by inhibiting MMP 2 and 9 and neutrophil elastase, as well as down-regulating TREM1 and NLRP3/caspase-1 signals during lung injury.

Despite our positive results, our study has several limitations. First, although intratracheal LPS is a common experimental model of ARDS, it does not fully recapitulate the complexity of human ARDS and its treatment (e.g., patient co-morbidities, indirect lung injury from sepsis, mechanical ventilation, vaso-pressors, etc.). Second, although intratracheal injection of nCMT-3 was effective in mice, it is difficult to predict whether aerosol administration would be effective in large animal models or human ARDS. Finally, we used a prophylactic or pre-injury dosing model in our experiments and did not fully establish the efficacy of post-injury nCMT-3 administration in our studies. However, preliminary experiments have shown that administration of nCMT-3 at 2 and 4 h after IT LPS significantly attenuates several markers of lung injury including proinflammatory cytokine levels (TNF- α , IL-1 β , and IL-6) in BALF (see supplemental data 6, <http://links.lww.com/SHK/B436>).

Despite these limitations, our data provides evidence that prophylactic administration of aerosolized nCMT-3 attenuates LPS-mediated lung injury and inflammation via multiple anti-inflammatory mechanisms including: MMP activation, PMN elastase, sTREM-1 release, and NLRP3 inflammasome/caspase-1 activation. Although the anti-inflammatory effects of nCMT-3 may appear to be somewhat “nonspecific,” they target clinically important pathways of lung injury in ARDS including MMP activation, the NLRP3 inflammasome/caspase-1 pathway and TREM-1 activation.

REFERENCES

- Han S, Mallampalli RK: The acute respiratory distress syndrome: from mechanism to translation. *J Immunol (Baltimore Md: 1950)* 194(3):855–860, 2015.
- Kirkwood KL, Golub LM, Bradford PG: Non-antimicrobial and antimicrobial tetracyclines inhibit IL-6 expression in murine osteoblasts. *Ann N Y Acad Sci* 878:667–670, 1999.
- Pruzanski W, Stefanski E, Vadas P, McNamara TF, Ramamurthy N, Golub LM: Chemically modified non-antimicrobial tetracyclines inhibit activity of phospholipases A2. *J Rheumatol* 25(9):1807–1812, 1998.
- Maitra SR, Shapiro MJ, Bhaduri S, El-Maghrabi MR: Effect of chemically modified tetracycline on transforming growth factor-beta1 and caspase-3 activation in liver of septic rats. *Crit Care Med* 33(7):1577–1581, 2005.
- Halter JM, Pavone LA, Steinberg JM, Gatto LA, DiRocco J, Landas S, Nieman GF: Chemically modified tetracycline (COL-3) improves survival if given 12 but not 24 hours after cecal ligation and puncture. *Shock* 26(6):587–591, 2006.
- Roy SK, Kubiak BD, Albert SP, Vieau CJ, Gatto L, Golub L, Lee HM, Sookhu S, Vodovotz Y, Nieman GF: Chemically modified tetracycline 3 prevents acute respiratory distress syndrome in a porcine model of sepsis + ischemia/reperfusion-induced lung injury. *Shock* 37(4):424–432, 2012.

7. Banik BL, Fattahi P, Brown JL: Polymeric nanoparticles: the future of nanomedicine. *Wiley Interdiscip Rev Nanomed Nanobiotechnol* 8(2):271–299, 2016.
8. Mitchell MJ, Billingsley MM, Haley RM, Wechsler ME, Peppas NA, Langer R: Engineering precision nanoparticles for drug delivery. *Nat Rev Drug Discov* 20(2):101–124, 2021.
9. Yang X, Zhao L, Almasy L, Garamus VM, Zou A, Willumeit R, Fan S: Preparation and characterization of 4-dedimethylamino sancycline (CMT-3) loaded nanostructured lipid carrier (CMT-3/NLC) formulations. *Int J Pharm* 450(1):225–234, 2013.
10. Luo J, Xiao K, Li Y, Lee JS, Shi L, Tan Y-H, Xing L, Hilland Cheng R, Liu GY, Lam KS: Well-defined, size-tunable, multifunctional micelles for efficient paclitaxel delivery for cancer treatment. *Bioconjug Chem* 21(7):1216–1224, 2010.
11. Borghardt JM, Kloft C, Sharma A: Inhaled therapy in respiratory disease: the complex interplay of pulmonary kinetic processes. *Can Respir J* 2018:2732017, 2018.
12. Videira MA, Llop J, Sousa C, Kreutzer B, Cossío U, Forbes B, Vieira I, Gil N, Silva-Lima B: Pulmonary administration: strengthening the value of therapeutic proximity. *Front Med* 7(50), 2020.
13. Lim GB: Drug delivery using inhaled nanoparticles. *Nat Rev Cardiol* 15(3):133, 2018.
14. Wang X, Shi C, Zhang L, Bodman A, Guo D, Wang L, Hall WA, Wilkens S, Luo J: Affinity-controlled protein encapsulation into sub-30 nm telodendrimer nanocarriers by multivalent and synergistic interactions. *Biomaterials* 101:258–271, 2016.
15. Shi C, Guo D, Xiao K, Wang X, Wang L, Luo J: A drug-specific nanocarrier design for efficient anticancer therapy. *Nat Commun* 6:7449, 2015.
16. Huang W, Wang X, Shi C, Guo D, Xu G, Wang L, Bodman A, Luo J: Fine-tuning vitamin E-containing telodendrimers for efficient delivery of gambogic acid in colon cancer treatment. *Mol Pharm* 12(4):1216–1229, 2015.
17. Busch CJ, Favret J, Geirsdotter L, Molawi K, Sieweke MH: Isolation and long-term cultivation of mouse alveolar macrophages. *Bio Protoc* 9(14), 2019.
18. Ortiz-Munoz G, Looney MR: Non-invasive intratracheal instillation in mice. *Bio Protoc* 5(12), 2015.
19. Matute-Bello G, Downey G, Moore BB, Groshong SD, Matthay MA, Slutsky AS, Kuebler WM: An official American Thoracic Society workshop report: features and measurements of experimental acute lung injury in animals. *Am J Respir Cell Mol Biol* 44(5):725–738, 2011.
20. Acharya MR, Venitz J, Figg WD: Sparreboom A: Chemically modified tetracyclines as inhibitors of matrix metalloproteinases. *Drug Resist Updat* 7(3):195–208, 2004.
21. Maitra SR, Bhaduri S, Valane PD, Tervahartiala T, Sorsa T, Ramamurthy N: Inhibition of matrix metalloproteinases by chemically modified tetracyclines in sepsis. *Shock* 20(3):280–285, 2003.
22. Carney DE, McCann UG, Schiller HJ, Gatto LA, Steinberg J, Picone AL, Nieman GF: Metalloproteinase inhibition prevents acute respiratory distress syndrome. *J Surg Res* 99(2):245–252, 2001.
23. Kim JH, Lee SY, Bak SM, Suh IB, Lee SY, Shin C, Shim JJ, In KH, Kang KH, Yoo SH: Effects of matrix metalloproteinase inhibitor on LPS-induced goblet cell metaplasia. *Am J Physiol Lung Cell Mol Physiol* 287(1). L127-33, 2004.
24. Maitra SR, Bhaduri S, Chen E, Shapiro MJ: Role of chemically modified tetracycline on TNF-alpha and mitogen-activated protein kinases in sepsis. *Shock* 22(5):478–481, 2004.
25. Steinberg J, Halter J, Schiller H, Gatto L, Carney D, Lee HM, Golub L, Nieman GF: Chemically modified tetracycline prevents the development of septic shock and acute respiratory distress syndrome in a clinically applicable porcine model. *Shock* 24(4):348–356, 2005.
26. Zhou X, Wang D, Ballard-Croft CK, Simon SR, Lee HM, Zwischenberger JB: A tetracycline analog improves acute respiratory distress syndrome survival in an ovine model. *Ann Thorac Surg* 90(2):419–426, 2010.
27. Weiss G, Lai C, Fife ME, Grabiec AM, Tildy B, Snelgrove RJ, Xin G, Liyod CM, Hussell T: Reversal of TREM-1 ectodomain shedding and improved bacterial clearance by intranasal metalloproteinase inhibitors. *Mucosal Immunol* 10(4):1021–1030, 2017.
28. Yuan Z, Syed MA, Panchal D, Rogers D, Joo M, Sadikot RT: Curcumin mediated epigenetic modulation inhibits TREM-1 expression in response to lipopolysaccharide. *Int J Biochem Cell Biol* 44(11):2032–2043, 2012.
29. Bouchon A, Dietrich J, Colonna M: Cutting edge: inflammatory responses can be triggered by TREM-1, a novel receptor expressed on neutrophils and monocytes. *J Immunol* 164(10):4991–4995, 2000.
30. Zheng H, Heiderscheidt CA, Joo M, Gao X, Knezevic N, Mehta D, Sadikot RT: MYD88-dependent and -independent activation of TREM-1 via specific TLR ligands. *Eur J Immunol* 40(1):162–71, 2010.
31. Sun J, Shigemitsu H, Tanaka Y, Yamauchi T, Ueda T, Iwasaki H: Tetracyclines downregulate the production of LPS-induced cytokines and chemokines in THP-1 cells via ERK, p38, and nuclear factor-kappaB signaling pathways. *Biochem Biophys Res Commun* 4:397–404, 2015.
32. Palmiere C, Augsburger M: Markers for sepsis diagnosis in the forensic setting: state of the art. *Croat Med J* 55(2):103–114, 2014.
33. Jedynak M, Siemiatkowski A, Mroczo B, Groblewska M, Milewski R, Szmitekowski M: Soluble TREM-1 serum level can early predict mortality of patients with sepsis, severe sepsis and septic shock. *Arch Immunol Ther Exp (Warsz)* 66(4):299–306, 2018.
34. Zhong WJ, Duan JX, Liu T, Yang HH, Guan XX, Zhang CY, Yang JT, Xiong JB, Zhou Y, Guan CX, et al.: Activation of NLRP3 inflammasome up-regulates TREM-1 expression in murine macrophages via HMGB1 and IL-18. *Int Immunopharmacol* 89(Pt A):107045, 2020.
35. Dolinay T, Kim YS, Howrylak J, Hunninghake GM, An CH, Fredenburgh L, Massaro AF, Rogers A, Gazourian L, Nakahira K, et al.: Inflammasome-regulated cytokines are critical mediators of acute lung injury. *Am J Respir Crit Care Med* 185(11):1225–1234, 2012.
36. Jones HD, Crother TR, Gonzalez-Villalobos RA, Jupelli M, Chen S, Dagvadorj J, Arditi M, Shimada K: The NLRP3 inflammasome is required for the development of hypoxemia in LPS/mechanical ventilation acute lung injury. *Am J Respir Cell Mol Biol* 50(2):270–280, 2014.
37. Peukert K, Fox M, Schulz S, Feuerborn C, Frede S, Putensen C, Wrigge H, Kummerer BM, David S, Seeliger B, et al.: Inhibition of caspase-1 with tetracycline ameliorates acute lung injury. *Am J Respir Crit Care Med* 204(1):53–63, 2021.
38. Lu Y, Xiao G, Luo W: Minocycline suppresses NLRP3 inflammasome activation in experimental ischemic stroke. *Neuroimmunomodulation* 23(4):230–238, 2016.
39. Liu T, Zhou Y, Li P, Duan JX, Liu YP, Sun GY, Wan L, Dong L, Fang X, Jiang JX, et al.: Blocking triggering receptor expressed on myeloid cells-1 attenuates lipopolysaccharide-induced acute lung injury via inhibiting NLRP3 inflammasome activation. *Sci Rep* 6:39473, 2016.

